# Sliding Mode Control of a Direct-Injection Monopropellant-Powered Actuator

Kevin B. Fite, Jason E. Mitchell, Eric J. Barth, and Michael Goldfarb

***Abstract*—** This paper describes the modeling and control of a direct-injection monopropellant-powered actuator. The actuation system utilizes the catalytic decomposition of a monopropellant, the products of which are directly injected into opposing chambers of a pneumatic cylinder in order to obtain a controllable force source. The system incorporates a pair of proportional liquid fuel valves and a three-way rotary spool valve to control the pressurization and depressurization of each chamber of the actuator. A model of the catalytic decomposition of the monopropellant and the compressible gas dynamics is derived in order to control the output force of the hot gas actuator. Using a Lyapunov function, a model-based sliding mode controller is developed for the multi-input single-output nonlinear system. Experimental results of the actuator force tracking demonstrate the validity of the model of the monopropellant-based actuator and the performance of the nonlinear controller.

## I. Introduction

One of the most significant challenges in the development of an autonomous human-scale robot is the issue of power supply. Perhaps the most likely power supply/actuator candidate system for a position or force actuated human-scale robot is an electrochemical battery and DC motor combination. This type of system, however, would have to carry an inordinate amount of battery weight in order to perform a significant amount of work for a significant period of time. A state-of-the-art example of a human-scale robot that utilizes electrochemical batteries combined with DC motor/harmonic drive actuators is the Honda Motor Corporation humanoid robot model P3. The P3 robot has a total mass of 130 kg (285 lb), 30 kg (66 lbs) of which are nickel-zinc batteries. These 30 kg of batteries provide sufficient power for approximately 15-25 minutes of operation, depending on its workload. Operation times of this magnitude are common in self-powered position or force controlled human-scale robots, and represent a major technological roadblock for designing actuated mobile robots that can operate power-autonomously for extended periods of time.

Manuscript received March 12, 2004.

K. B. Fite, J. E. Mitchell, E. J. Barth and M. Goldfarb are with the Department of Mechanical Engineering, Vanderbilt University, Nashville, TN 37235 USA (e-mail: kevin.fite@vanderbilt.edu; jason.mitchell@vanderbilt.edu, barthej@vuse.vanderbilt.edu; goldfarb@vuse.vanderbilt.edu;).

## II. Monopropellant Approach

Liquid chemical fuels can provide energy densities significantly greater than power-comparable electrochemical batteries. The energy from these fuels, however, is released as heat, and the systems required to convert heat into controlled, actuated work are typically complex, heavy, and inefficient. One means of converting chemical energy into controlled, actuated work with a simple conversion process is to utilize a liquid monopropellant to generate a gas, which in turn can be utilized to power a pneumatic actuation system. Specifically, monopropellants are a class of fuels (technically propellants since oxidation doesn't occur) that rapidly decompose (or chemically react) in the presence of a catalytic material. Unlike combustion reactions, no ignition is required, and therefore the release of power can be controlled continuously and proportionally simply by controlling the flow rate of the liquid propellant. This results in a simple, low weight energy converter system, which provides a good solution to the design trade-offs between fuel energy density and system weight for the scale of interest.

Monopropellants, originally developed in Germany during World War II, have since been utilized in several applications involving power and propulsion, most notably to power gas turbine and rocket engines for underwater and aerospace vehicles. Modern day applications include torpedo propulsion, reaction control thrusters on a multitude of space vehicles, and auxiliary power turbo pumps for aerospace vehicles. Despite the use of monopropellants in these various applications, the authors have not been able to find any prior literature describing the development of position or force controllable monopropellant-powered actuators. The only indication of prior related work is the patent by Morash [1], which describes a pilot-operated binary valve that utilizes a monopropellant in the pilot stream.

The test bed consists of a direct-injection chemofluidic actuator powering a single-degree-of-freedom arm, and is shown in Figure 1. Note that the arm is holding a 25 lb

weight. The actuator shown in Figure 1 embodies a direct-injection configuration, which utilizes the direct injection of a liquid monopropellant into the respective chambers of a linear cylinder, as illustrated in the schematic of Figure 2. A monopropellant is a substance that undergoes a strongly exothermic reaction upon contact with a catalyst. In the direct-injection configuration, a liquid monopropellant is injected on-demand through the catalyst packs and into the respective sides of the cylinder actuator. The mechanical power output of the piston results from the combined effects of the liquid propellant inlet flow and gaseous exhaust outlet flow.

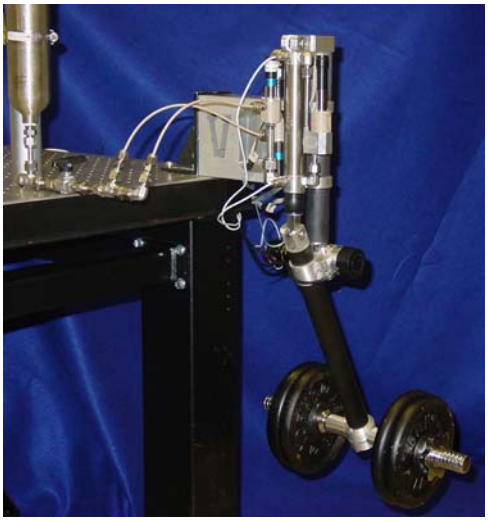

Fig. 1. Direct-injection actuated single degree-of-freedom manipulator prototype holding a 25 lb weight.

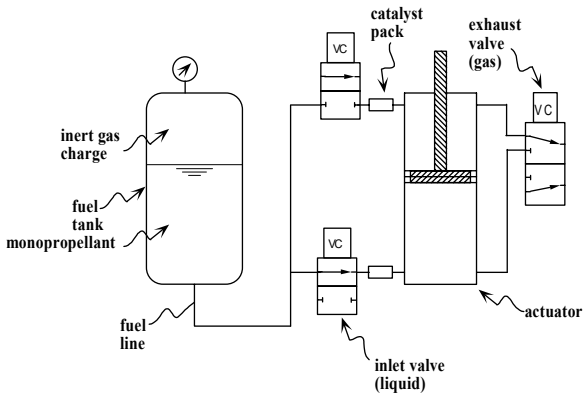


Fig. 2. Schematic representation of the direct-injection cheomfluidic actuator.

The control of these actuators is markedly different from standard types of actuators and as such requires the development of unique approaches to their motion and force control. In particular, these actuators are characterized by highly nonlinear gas dynamics and chemical reaction dynamics inside the control loop. Additionally, they are generally multi-input single-output. In addition to providing several control challenges, successful implementation must combine the objectives of control performance with objectives of high energy conversion efficiency (i.e., the actuators must not only demonstrate good tracking performance, but must also demonstrate a high energy density). The primary objective of this work is to develop the control framework necessary to address issues of control in these high energy density actuators.

## III. Equations of Motion

### A. Catalytic Decomposition Equations

The dynamics governing the catalytic decomposition of the monopropellant are derived by considering a control volume around the catalyst pack and using a power balance relating the rate of energy storage to the energy flux rate across the boundary of the control volume, as detailed by Barth, et al. [2]. Assuming the rate of work done to the environment is zero and the rate of internal energy in the catalyst pack is negligible compared to that of the actuator chamber, the mass flow rate of compressible gas leaving the catalyst chamber (i.e., the mass flow rate of gas entering the actuator chamber) is given by:

$$\dot{m}_{in} = \frac{1}{C_p T_{ADT}} \dot{Q}_r \tag{1}$$

where $C_p$ is the specific heat at constant pressure, $T_{ADT}$ is the adiabatic decomposition temperature of the monopropellant, and $\dot{Q}_r$ is rate of heat released by the monopropellant. The heat released by the isentropic decomposition is modeled as the following first order dynamic:

$$\tau_r \ddot{Q}_r + \dot{Q}_r = k\dot{m}_{fuel} \tag{2}$$

where $\tau_r$ is the time constant, $k$ is the heat of decomposition minus the heat of vaporization of the product liquids, and $\dot{m}_{fuel}$ is the mass flow rate of monopropellant into the catalyst pack. The mass flow rate of liquid monopropellant is governed by the standard hydraulic flow equation for a liquid thru an orifice, given by:

$$\dot{m}_{fuel} = c u_{in} \sqrt{2\rho_L (P_s - P)} \tag{3}$$

where $c$ is the discharge coefficient of the liquid fuel valve, $u_{in}$ is the area of the valve orifice, $\rho_L$ is the density of the liquid monopropellant, $P_s$ is the supply pressure, and $P$ is the downstream pressure.

### B. Discharge Equations

The mass flow rate leaving the actuator chamber is governed by the dynamics of compressible fluid flow thru an orifice, determined based on the pressures inside and outside the actuator chamber. Under isentropic flow assumptions, the mass flow rate through the exhaust valve orifice is determined by:

$$\dot{m}_{out} = \Psi(P) u_{out} \tag{4}$$

where $u_{out}$ is the area of the exhaust valve orifice and $\Psi(P)$ is the normalized mass flow rate. The normalized mass flow rate will reside in the sonic (choked) or subsonic (unchoked) flow regime, and is given by:

$$\Psi(P)=\begin{cases}\dfrac{C_1 C_f P}{\sqrt{T_{ADT}}} & \text{if } \dfrac{P_{atm}}{P}\le C_r \text{ (choked)}\\ \dfrac{C_2 C_f P}{\sqrt{T_{ADT}}}\left(\dfrac{P_{atm}}{P}\right)^{(1/\gamma)}\sqrt{1-\left(\dfrac{P_{atm}}{P}\right)^{(\gamma-1)/\gamma}} & \text{otherwise (unchoked)}\end{cases} \quad (5)$$

where $C_f$ is the discharge coefficient of the exhaust valve, $P$ and $P_{atm}$ are the upstream and downstream pressures, respectively, $\gamma$ is the ratio of specific heats, $C_r$ is the pressure ratio governing the transition between sonic and subsonic flow regimes, and $C_1$ and $C_2$ are constants defined by:

$$C_1=\sqrt{\frac{\gamma}{R}\left(\frac{2}{\gamma+1}\right)^{(\gamma+1)/(\gamma-1)}} \quad (6)$$

$$C_2=\sqrt{\frac{2\gamma}{R(\gamma-1)}} \quad (7)$$

where $R$ is the universal gas constant.

### C. Actuator Force

The goal of the monopropellant powered actuator is to provide a controllable force source, where the force generated by the actuator is given by:

$$F_{act}=P_A A_A - P_B A_B - P_{atm} A_r \quad (8)$$

where $P_A$ and $P_B$ are the pressures in chambers $A$ and $B$, respectively, $P_{atm}$ is the atmospheric pressure, $A_A$ and $A_B$ are the effective areas of each side of the piston, and $A_r$ is the cross-sectional area of the piston rod. The rates of pressure in each chamber, under the assumption of isentropic flow, are governed by:

$$\dot{P}_{(A,B)}=\frac{\gamma R T_{ADT}}{V_{(A,B)}}\dot{m}_{(A,B)}-\frac{\gamma P_{(A,B)}}{V_{(A,B)}}\dot{V}_{(A,B)} \quad (9)$$

where $P_{(A,B)}$ is the pressure inside each cylinder chamber, $\dot{m}_{(A,B)}$ is the mass flow rate into or out of each side of the cylinder, and $V_{(A,B)}$ is the volume of each chamber.

The actuator is constrained to operate in one of two modes: (1) charging chamber A and exhausting chamber B or (2) exhausting chamber A and charging chamber B. In mode 1 ($u_{in}$, $u_{out} \ge 0$), the mass flow rates of compressible gas in chambers A and B, respectively, are determined by:

$$\dot{m}_A=\dot{m}_{in,A}=\frac{1}{C_p T_{ADT}}\dot{Q}_{r,A} \quad (10)$$

$$\dot{m}_B=\dot{m}_{out,B}=-\Psi(P_B)u_{out} \quad (11)$$

where the heat release of the catalyst pack connected to chamber A is governed by:

$$\tau_r\ddot{Q}_{r,A}+\dot{Q}_{r,A}=kcu_{in}\sqrt{2\rho_L(P_s-P_A)} \quad (12)$$

Similarly, for operation in mode 2 ($u_{in}$, $u_{out} < 0$), the mass flow rates in each cylinder chamber are:

$$\dot{m}_A=\dot{m}_{out,A}=\Psi(P_A)u_{out} \quad (13)$$

$$\dot{m}_B=\dot{m}_{in,B}=\frac{1}{C_p T_{ADT}}\dot{Q}_{r,B} \quad (14)$$

and the heat release of the catalyst pack for chamber B is determined by:

$$\tau_r\ddot{Q}_{r,B}+\dot{Q}_{r,B}=-kcu_{in}\sqrt{2\rho_L(P_s-P_B)} \quad (15)$$

## IV. Actuator Control

The control approach for the direct-injection monopropellant-powered actuator utilizes a model-based controller derived using an appropriate Lyapunov function. Nonlinear model-based control methodologies are based upon system dynamics that are square (i.e., an input for each output) and expressable in control canonical form (i.e., the control inputs appear in the highest order state equation). With respect to the monopropellant-powered actuator however, the dynamics are both non-square (actuator force is affected by both inlet and exhaust valve areas) and non-control canonical (inlet valve area appears in higher-order state equation than the exhaust valve area). In order to address these issues, a constraint equation is implemented in order to determine the exhaust valve area as a function of the inlet valve area. Using the constraint discussed in the following section, the dynamics of the actuator reduce to a single-input single-output system to which the sliding mode control methodology can then be directly applied to determine the desired liquid valve area.

### A. Constraint Between Inlet and Exhaust Valve Areas

In order to constrain the system dynamics in mode 1, in which chamber B is exhausted, the exhaust mass flow rate of chamber B is determined based on the inlet mass flow rate of chamber A using the following constraint:

$$\dot{P}_{B,d}=-\dot{P}_A \quad (16)$$

where $\dot{P}_{B,d}$ is the desired rate of pressure in chamber B. The mass flow rate of chamber B is then given by:

$$\dot{m}_B=\dot{m}_{B,\max}\text{sat}\left(\frac{\dot{m}_{B,d}}{\dot{m}_{B,\max}}\right) \quad (17)$$

where $\dot{m}_{B,d}$ is the desired mass flow rate of chamber B, $\dot{m}_{B,\max}$ is the maximum attainable mass flow rate of chamber B, and sat(*) is the saturation function. The mass flow rate of gas leaving chamber B, as defined in eqn. 17, accounts for the physical limitations of the exhaust valve. As such, when the exhaust valve can satisfy the constraint of eqn. 16, it does so. Otherwise, the exhaust valve provides it maximum attainable mass flow rate. The desired mass flow rate of chamber B is obtained by combining equations (9) and (16), such that:

$$\dot{m}_{B,d}=\frac{V_B}{RT_{ADT}}\left(\frac{P_A\dot{V}_A}{V_A}+\frac{P_B\dot{V}_B}{V_B}\right)-\frac{V_B}{V_A}\dot{m}_A \quad (18)$$

The maximum mass flow rate is determined, assuming

sonic (choked) flow, by:

$$\dot{m}_{B,\max} = -u_{out,\max}\Psi(P_B)_{choked} \tag{19}$$

where $u_{out,max}$ is the maximum orifice area of the exhaust valve. In order to facilitate the Lyapunov control design, a continuously differentiable expression for $\dot{m}_B$ is needed. The saturation function is approximated using the arctangent function such that:

$$\dot{m}_B = \dot{m}_{B,\max}\left(\frac{2}{\pi}\right)\tan^{-1}\left(\beta\frac{\dot{m}_{B,d}}{\dot{m}_{B,\max}}\right) \tag{20}$$

The parameter β determines the slope of the approximation to the saturation function, and is defined by:

$$\beta = \beta_o + \mu(P_A + P_B - 2\overline{P}) \tag{21}$$

where $\beta_o$ is the initial value for β, μ is a strictly positive constant, and $\overline{P}$ is the desired average pressure in each cylinder chamber. As the average pressure deviates from the desired, β changes to provide more or less exhaust authority as needed. The constraint equations for mode 2, in which chamber A is exhausted, are analogous to that for mode 1. The governing constraint equations for mode 2 are obtained from equations (16)-(21) by switching the subscripts A and B.

### *B. Sliding Mode Control Law*

To implement a control law based on a Lyapunov function, the expression for actuator force of equation (8) must be differentiated until the control input ($u_{in}$) appears directly. The area of the liquid fuel valve appears in the expressions for $\ddot{P}_A$ and $\ddot{P}_B$, and thus, in order to apply the Lyapunov-based control methodology, the expression for actuator force must be differentiated twice yielding:

$$\ddot{F}_{act} = \ddot{P}_A A_A - \ddot{P}_B A_B \tag{22}$$

where

$$\ddot{P}_{(A,B)} = \frac{\gamma RT_{ADT}}{V_{(A,B)}}\ddot{m}_{(A,B)} - \frac{\gamma RT_{ADT}\dot{V}_{(A,B)}}{V^2_{(A,B)}}\dot{m}_{(A,B)} - \frac{\gamma(P\ddot{V}+\dot{P}\dot{V})_{(A,B)}}{V_{(A,B)}} + \frac{\gamma(P\dot{V}^2)_{(A,B)}}{V_{(A,B)}} \tag{23}$$

Using the appropriate expressions for mass flow rates and rates of pressure, equation (23) can be written in the following condensed form:

$$\ddot{P}_{(A,B)} = f_{(A,B)}(\mathbf{x}) + b_{(A,B)}(\mathbf{x})u_{in} \tag{24}$$

where $f_{(A,B)}(\mathbf{x})$ and $b_{(A,B)}(\mathbf{x})$ are state-dependent equations obtained by appropriate differentiation of the plant dynamics. The Lyapunov function for the dynamics as expressed by equation (22) is given by the sliding surface:

$$s = \dot{F}_{act} - \dot{F}_{act,d} + \lambda(F_{act} - F_{act,d}) \tag{25}$$

where $F_{act,d}$ is the desired actuator force and λ is a strictly positive constant. The control input is determined by forcing $\dot{s} = 0$ and solving for $u_{in}$. The resulting equivalent control law enhanced with a robustness term of the form -K*sat(s/Φ) ensures that the derivative of the Lyapunov function of equation (25) is negative definite.

Operation in mode 1 incorporates the dynamics of charging chamber A with those of the constrained exhaust of chamber B. The expressions governing the pressure dynamics for each chamber are given by:

$$\ddot{P}_A = f_{A,1}(\mathbf{x}) + b_{A,1}(\mathbf{x})u_{in} \tag{26}$$

$$\ddot{P}_B = f_{B,1}(\mathbf{x}) + b_{B,1}(\mathbf{x})u_{in} \tag{27}$$

The control law for the area of the liquid fuel valve in mode 1 is given by:

$$u_{in,1} = \begin{cases} u_{in,1eq} - K\,\mathrm{sat}(\frac{s}{\Phi}) & \text{if } u_{in,1} \geq 0 \\ 0 & \text{otherwise} \end{cases} \tag{28}$$

where $K$ is a strictly positive gain, Φ is the boundary layer thickness, and $u_{in,1eq}$ is the equivalent control law defined by:

$$u_{in,1eq} = \frac{1}{A_A b_{A,1}(\mathbf{x}) - A_B b_{B,1}(\mathbf{x})}\begin{bmatrix}\ddot{F}_{act,d} - \lambda(\dot{F}_{act} - \dot{F}_{act,d}) \\ -A_A f_{A,1}(\mathbf{x}) + A_B f_{B,1}(\mathbf{x})\end{bmatrix} \tag{29}$$

The area of the exhaust valve is then obtained from the area of the liquid fuel valve using:

$$u_{out,1} = \begin{cases} -\dfrac{\dot{m}_B}{\Psi_B} & \text{if } u_{out,1} \geq 0 \\ 0 & \text{otherwise} \end{cases} \tag{30}$$

where $\dot{m}_B$ is defined by the constraint of equations (16)-(21). In this form, the fuel and exhaust valves are nonzero only when the resulting valve areas are positive.

Actuator operation in mode 2 is characterized by exhausting chamber A and charging chamber B, with the pressure dynamics written as:

$$\ddot{P}_A = f_{A,2}(\mathbf{x}) + b_{A,2}(\mathbf{x})u_{in} \tag{31}$$

$$\ddot{P}_B = f_{B,2}(\mathbf{x}) + b_{B,2}(\mathbf{x})u_{in} \tag{32}$$

The area of the liquid fuel valve in mode 2 is then given by:

$$u_{in,2} = \begin{cases} u_{in,2eq} - K\,\mathrm{sat}(\frac{s}{\Phi}) & \text{if } u_{in,2} < 0 \\ 0 & \text{otherwise} \end{cases} \tag{33}$$

and the equivalent control law is:

$$u_{in,2eq} = \frac{1}{A_A b_{A,1}(\mathbf{x}) - A_B b_{B,1}(\mathbf{x})}\begin{bmatrix}\ddot{F}_{act,d} - \lambda(\dot{F}_{act} - \dot{F}_{act,d}) \\ -A_A f_{A,1}(\mathbf{x}) + A_B f_{B,1}(\mathbf{x})\end{bmatrix} \tag{34}$$

The exhaust valve area is then determined as a function of $u_{in,2}$ using:

$$u_{out,2} = \begin{cases} \dfrac{\dot{m}_A}{\Psi_A} & \text{if } u_{out,2} < 0 \\ 0 & \text{otherwise} \end{cases} \tag{35}$$

where $\dot{m}_A$ is the constrained mass flow rate of chamber A obtained equations analogous to those of equations (16)-(21), but applied to exhausting chamber A. The fuel and exhaust valves for mode 2 are nonzero only when the

resulting valve areas are negative. The areas commanded to the fuel and exhaust valves are then given by:

$$u_{in} = u_{in,1} + u_{in,2} \tag{36}$$

$$u_{out} = u_{out,1} + u_{out,2} \tag{37}$$

Note that due to the definition of $u_{in}$ and $u_{out}$ in each mode, only the areas for a single mode will be nonzero at any given instant.

## V. Simulation and Experimental Results

In order to assess the performance of the sliding mode control of the monopropellant-powered actuator, simulations of force control of the single degree-of-actuator are conducted for conditions of fixed actuator volume and parametric error of 20% in each parameter of the sliding mode controller. These simulations serve to verify the performance of the model-based controller and allow for tuning of the control parameters prior to conducting any experiments with the energy-dense liquid monopropellant. Figures (3)-(6) show the results of force tracking for sinusoidal frequencies of 0.25, 0.5, 1 and 2 Hz with an amplitude of 200N. The simulated results indicate that the Lyapunov-based force control law provides sufficient robustness to exhibit good tracking performance even in the presence of significant uncertainty.

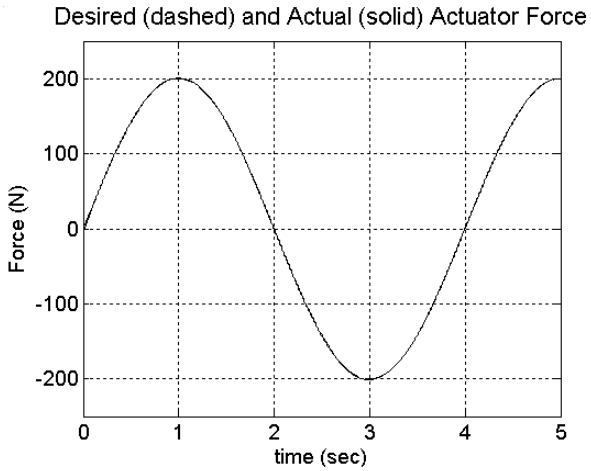


Fig. 3. Simulation of actuator force tracking at 0.25 Hz with 20% parametric error.

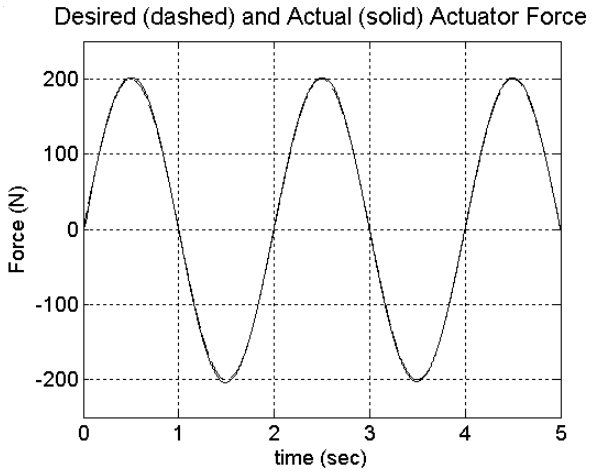


Fig. 4. Simulation of actuator force tracking at 0.5 Hz with 20% parametric error.

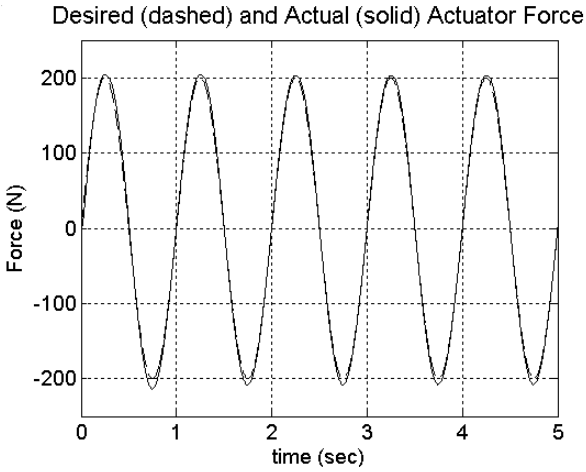


Fig. 5. Simulation of actuator force tracking at 1 Hz with 20% parametric error.

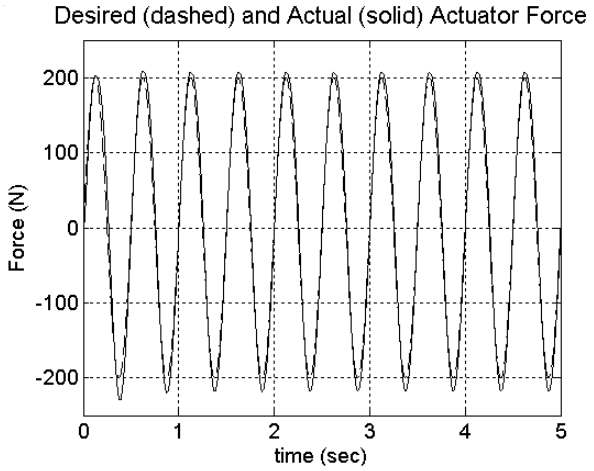


Fig. 6. Simulation of actuator force tracking at 2 Hz with 20% parametric error.

Following the simulations, experimental tests for force tracking of the monopropellant-powered actuator were then conducted under analogous conditions to the simulations (i.e., 200N amplitude, fixed chamber volume, identical control gains). Figures (7)-(10) show the experimental results of force tracking of the actuator using 70% hydrogen peroxide as the liquid monopropellant. The force tracking experiments were conducted for frequencies of 0.25, 0.5, 1, and 2 Hz, and the results of the experiments are comparable to those predicted by simulation.

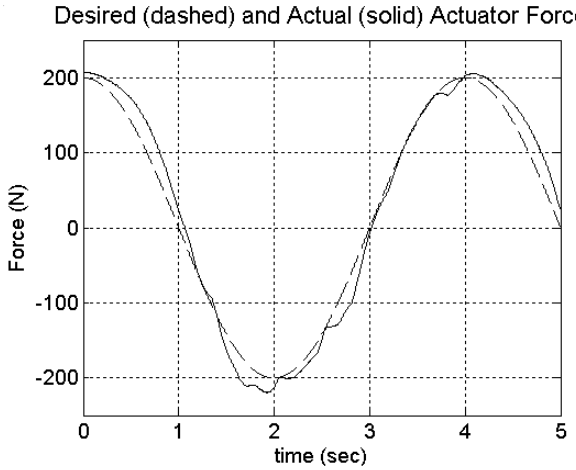

Fig. 7. Experimental actuator force tracking at 0.25 Hz.

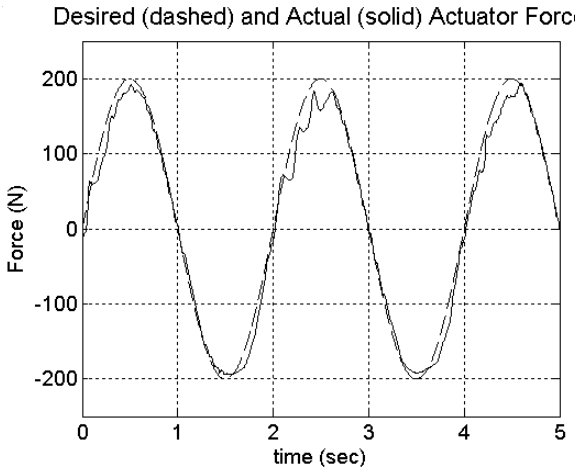

Fig. 8. Experimental actuator force tracking at 0.5 Hz.

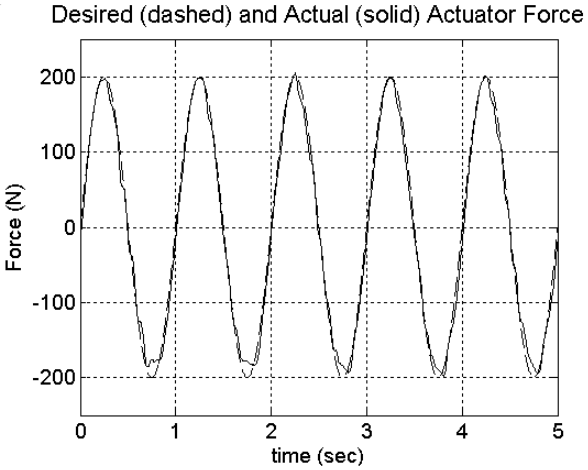

Fig. 9. Experimental actuator force tracking at 1 Hz.

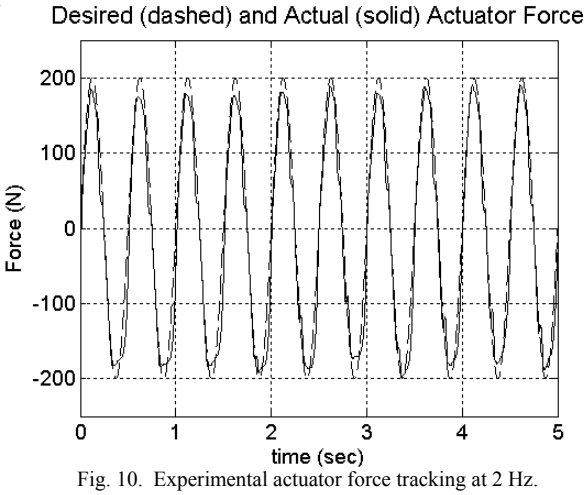

Fig. 10. Experimental actuator force tracking at 2 Hz.

## VI. Conclusion

The goal of this paper is the derivation of a nonlinear model-based sliding mode controller for the purposes of force control of a hot gas actuator powered with a liquid monopropellant. The simulation and experimental results of actuator force control validate the derived nonlinear model-based control of the monopropellant-powered actuator. Having demonstrated good force control, the monopropellant-powered hot gas actuator can be utilized in numerous applications requiring a self-powered force source for controlled mechanical work.

## References

[1] Morash, D.H., Hypergolic/Catalytic Actuator. United States patent 4,825,819, 1989.

[2] Barth, E.J., Gogola, M.A., and Goldfarb, M., "Modeling and Control of a Monopropellant-Based Pneumatic Actuation System," *Proceedings of 2003 IEEE International Conference on Robotics and Automation,* vol. I, pp. 628-633, 2003.